

Structural and radiative evolution in quantum dots near the $\text{In}_x\text{Ga}_{1-x}\text{As}/\text{GaAs}$ Stranski-Krastanow transformation

R. Leon*

Research School of Physical Sciences, Australian National University, Australian Capital Territory 0200, Australia

S. Fafard

Institute for Microstructural Sciences, National Research Council, Ottawa, Ontario, Canada K1A 0R6

(Received 27 January 1998)

The evolution of Stranski-Krastanow (SK) quantum-dot (QD) formation in ternary $\text{In}_{0.6}\text{Ga}_{0.4}\text{As}/\text{GaAs}$ was studied with graded structures grown via organometallic vapor-phase epitaxy. Surface-probe microscopy showed island evolution between 3.5- and 6.5-monolayer (ML) deposition. Island densities increased exponentially (over three decades with 0.2-ML deposition) before saturation ~ 4.7 ML. Photoluminescence (PL) of capped structures show that the wetting-layer PL energy does not shift beyond the onset of the SK transition. PL intensities increased with QD concentration but not in proportion to QD density. After saturation, a sharp drop in PL intensity was observed, which we attribute to island coalescence and incoherent island formation. Excitation power dependence of the luminescence at different stages of QD evolution indicates a concentration dependence of optical saturation in self-forming $\text{In}_x\text{Ga}_{1-x}\text{As}$ QD's. [S0163-1829(98)50828-4]

Aims for a clearer understanding of the mechanisms in Stranski-Krastanow (SK) quantum dot (QD) self-formation bring forth several unresolved issues in the progression of structural and radiative QD evolution. Studies in numerous SK heteroepitaxial systems concur in the observation of a wetting layer (WL) forming before strained coherent islanding.^{1,2} However, the structural integrity of this wetting layer, its thickness and stability are not well understood. Some of the rapid increase in island formation could occur at the expense of a thinning WL that might be partially consumed by the islands/dots. Other issues of interest in the evolution of SK QD's are the relationship between radiative emission from WL and QD structures, and a quantitative determination of the radiative emission per QD. Furthermore, the effects of growth beyond saturation island densities (island coalescence) on radiative recombination have not been examined. Structures with $\text{In}_x\text{Ga}_{1-x}\text{As}$ deposition beyond island saturation are incorporated into QD devices to obtain emission at longer wavelengths,^{1,2} making this issue relevant from a technological perspective.

In the present study, we have investigated the evolution of SK island formation in a ternary ($\text{In}_x\text{Ga}_{1-x}\text{As}$) from two-dimensional (2D) growth until the onset of island coalescence. Gradients in quantum dot density can be produced by MOCVD by varying the carrier gas (H_2) flow. Structures with simulations of concentration profiles³ and shifts in the optical emission from thin quantum wells were used to obtain an equivalent scale in monolayers (ML's) deposition for this technique. This allowed determination of the two-dimensional (2D) to three-dimensional (3D) transition for $\text{In}_{0.6}\text{Ga}_{0.4}\text{As}/\text{GaAs}$ in a fashion similar to that reported by Leonard, Pond, and Petroff⁴ and Kobayashi *et al.*⁵ for InAs/GaAs . Our experiments demonstrate a similar exponential behavior in ternary $\text{In}_x\text{Ga}_{1-x}\text{As}/\text{GaAs}$ dot formation. Furthermore, correlating the structural and luminescence results showed the photoluminescence (PL) evolution from initial WL growth to QD formation, island saturation, and the effects of coalescence and incoherent island formation on QD

PL emission. Investigation of these graded structures also showed some effects of varying QD concentration, or dot-dot interaction, on the optical emission intensity and saturation behavior of $\text{In}_x\text{Ga}_{1-x}\text{As}$ QD's.

$\text{In}_x\text{Ga}_{1-x}\text{As}/\text{GaAs}$ structures were grown by metal-organic chemical-vapor deposition (MOCVD). A horizontal reactor operating at 76 Torr and $(\text{CH}_3)_3\text{Ga}$, $(\text{CH}_3)_3\text{In}$, and AsH_3 were used as precursors. The H_2 carrier flow rate used was 5 standard liters/min (slm), which gave spatially graded deposition. The flow of $(\text{CH}_3)_3\text{In}$ was monitored and controlled by an EPISON ultrasonic sensor. After growth of GaAs buffer layers at 650 °C, the temperature was lowered to 550 °C and nanometer-sized $\text{In}_x\text{Ga}_{1-x}\text{As}$ islands were grown by depositing ~ 5 ML of $\text{In}_{0.6}\text{Ga}_{0.4}\text{As}$. These nominal compositions were determined from PL measurements in thick relaxed films and PL emission from thin $\text{In}_x\text{Ga}_{1-x}\text{As}/\text{GaAs}$ quantum wells (QW's). Growth rates ranged from 0.5 to 0.75 ML/s. GaAs capping layer thicknesses were 30 nm (not graded). Substrates were (100) semi-insulating GaAs.

Force microscopy (FM) with standard etched silicon nitride tips was used to obtain statistical information on island surface densities. Similar experiments and prior work comparing FM and transmission electron microscope images indicate that concentrations in capped and uncapped samples are equivalent while sizes may vary.

Low (77 K) temperature photoluminescence (PL) spectra were obtained using the 532 nm continuous-wave output of a diode-pumped Nd:YVO₄ for excitation. Some spectra were collected using below band-gap (and below WL) excitation, using a 980-nm infrared laser diode. The signal was dispersed with a single grating 0.67-m monochromator, and collected using a cooled Ge detector and lock-in techniques.

Figure 1 shows the island concentration as a function of coverage in units of ML's. The deposition scale and gradients have been calibrated in this work by measurements of the PL emission and the corresponding shifts as a function of distance from graded $\text{In}_x\text{Ga}_{1-x}\text{As}/\text{GaAs}$ capped quantum

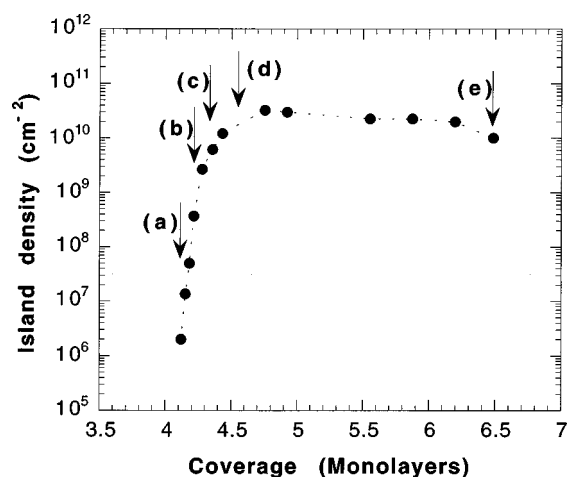


FIG. 1. Evolution in island concentration over depositions between 4.0 and 6.5 ML. Arrows at different stages of growth indicate representative structures shown in Fig. 2.

wells. The latter structures were grown under the same conditions as the graded QD samples but a shorter deposition time was used so the SK transformation did not occur in the wafer strip. This allowed establishing a growth rate in ML's as a function of distance from the edge of the MOCVD susceptor. From Fig. 1, we determined the critical thickness for the 2D to 3D transition in the MOCVD growth of $\text{In}_{0.6}\text{Ga}_{0.4}\text{As}$ to occur after 4.0-ML deposition. The onset of island coalescence becomes apparent with the decrease in island concentration with further deposition. These structural changes can also be appreciated in Fig. 2, which shows the progression in island density and surface morphology from the onset of island formation to growth past the SK transformation. The morphology indicated in each frame corresponds to the stages indicated by arrows in Fig. 1. The surface of the samples outside the islands was slightly rougher in structure than previously studied samples where the growth was performed with a higher H_2 flux. This might explain the broader emission coming from both 0D and 2D structures presented in our PL spectra (Figs. 3 and 4).

From Fig. 3 it can be seen that the evolution of the luminescence spectra from these structures can be divided into four distinct regions, labeled (a)–(d) in Fig. 3: WL emission,

simultaneous WL and QD emission, QD saturation, and last, the dislocation/coalescence regime.

Luminescence emission begins with a thin QW that progressively redshifts (becomes thicker) as $\text{In}_x\text{Ga}_{1-x}\text{As}$ deposition is increased. This is indicated in the lower portion of Fig. 3. In the next stage, the QD concentration rises until the threshold for QD PL detection. Once the QD PL peak increases in intensity, the WL peak diminishes rapidly. The evolution of WL to QD luminescence occurs over a broad range in QD concentrations but this corresponds to a very narrow range in $\text{In}_x\text{Ga}_{1-x}\text{As}$ deposition: from 4.08 to 4.14 ML. At the next stage, which occurs over the next ~ 0.5 -ML deposition, the PL QD emission does not change significantly. This stage corresponds to island saturation. In the last stage, the PL intensity drops in magnitude to roughly a third of its former intensity, and stays at this lower intensity over the next ~ 2 -ML deposition.

It can be seen from the spectra in Fig. 3(b) that PL emission intensities from QD's increase as their concentration increases, and that the WL emission is reduced. However, the energy of the WL PL peak stays at the same value once the QD PL peak becomes detectable and grows. The WL thickness then does not increase (or decrease) with further $\text{In}_x\text{Ga}_{1-x}\text{As}$ deposition once the QD start forming. We believe that what we observe is one of the possible mechanisms that can take place in QD formation, but that thinning "sacrificial" WL's can be observed under different growth conditions, namely, surfactant mediated growth.^{6,7}

Figure 3 also shows slight shifts in the PL emission line from QD's. The shifts before island saturation might have different origins than the ones seen after island saturation. After island saturation, extra deposited material is added to the existing islands, increasing their thickness. This would cause a redshift. Upon further deposition, islands are seen to coalesce, which would account for even greater redshifts. Before saturation, the PL QD emission is slightly redshifted with respect to the peak position at saturation. TEM examination of the dot sizes shows that sizes do not change before saturation.⁸ Therefore, we believe that the change in peak position is due to strain from neighboring dots getting closer as the QD concentration increases. Figure 5 shows plots of integrated PL and WL emission over the different structural

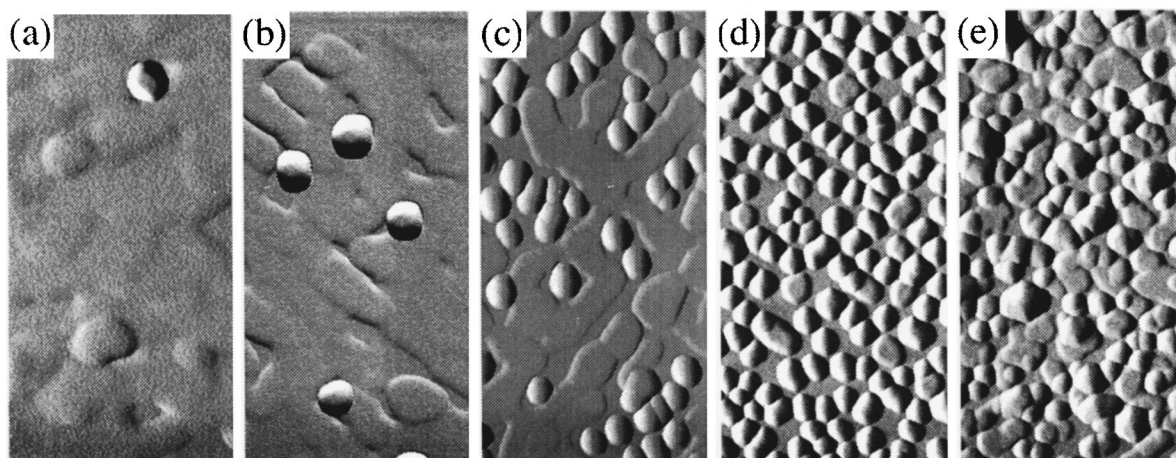


FIG. 2. Deflection FM images of surface evolution for $\text{In}_x\text{Ga}_{1-x}\text{As}/\text{GaAs}$ islands at the points indicated by arrows in Fig. 1. Each frame is $1 \times 0.5 \mu\text{m}$.

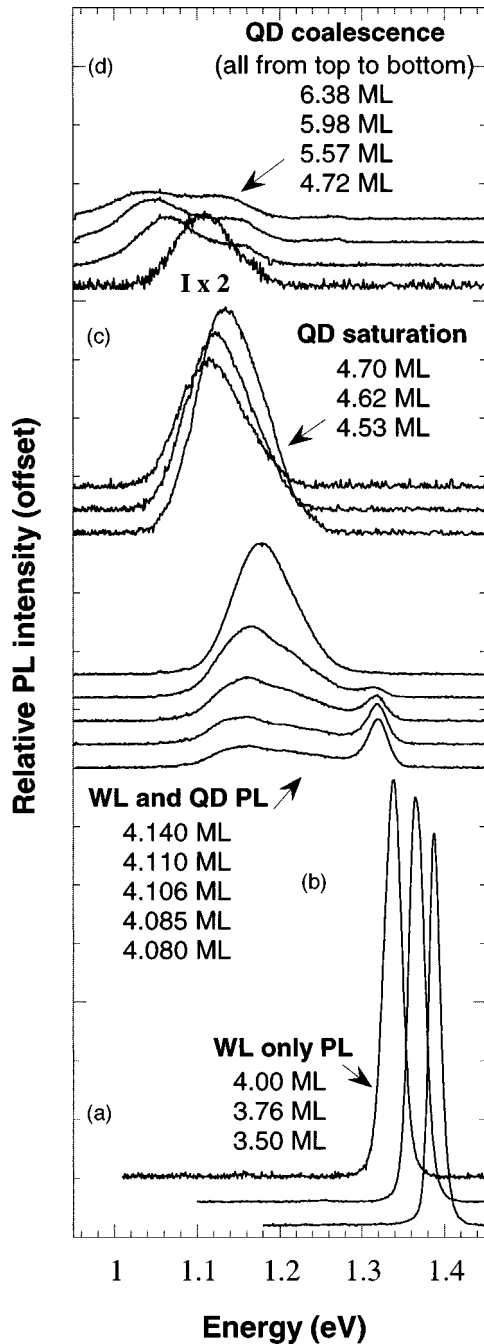


FIG. 3. PL spectra and calibrated relative intensities in different regimes of QD formation. (a) WL PL shifts before QD formation, (b) evolution of PL spectra at low QD densities when both QD and WL peaks are simultaneously observed, (c) strongest PL integrated intensity near island saturation, and (d) weak PL emission seen after island saturation and coalescence.

transformations taking place. Calibrated integrated PL intensities are shown for WL peaks, and for QD peaks with above and below band-gap excitation. This shows that although the total QD PL intensity increases with deposition, the PL per QD drops with increasing QD concentration. One possible explanation for this change is that when the QD density is low, the carrier/exciton diffusion from WL to QD's is very efficient, and the QD's receive more carriers. When the QD concentration is larger, this is decreased due to a smaller QD separation. For a fixed laser excitation power, the same num-

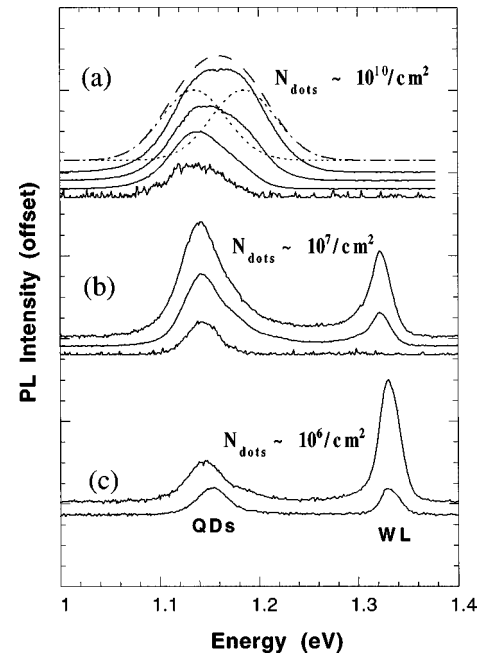


FIG. 4. Excitation power dependence of PL signal showing emission from QD and WL states for different values of QD areal concentrations. (a) The power excitation ratios for the solid lines are 192/64/6.4/0.192 W/cm². Simulations adding two Gaussian curves centered at $E_i = 1.135$ and 1.185 eV with 65-meV inhomogeneous broadening are shown separately in dashed lines. (b) Excitation power ratios 192/19.2/0.192 W/cm² and (c) power ratios 192/1.92 W/cm².

ber of carriers are then distributed over more QD's, with each QD receiving less carriers and producing a lower emission intensity. This does not explain the results with below band-gap excitation. In this case, the reason for this decrease is most likely due to dot-dot interactions or strain due to closely spaced dots. So either some dots become optically inactive, or the average emission per dot is lower. Further experiments using micro PL to examine the changes in PL emission from isolated dots will be necessary to further clarify this change in PL intensity per dot.

The sudden drop in PL intensity after island saturation is also apparent in Fig. 5, and it occurs over a very narrow range in deposition. Structural surface examination shows that the small number of large incoherent islands seen in $\text{In}_x\text{Ga}_{1-x}\text{As}/\text{GaAs}$ QD samples increase sharply, both in size and concentration, at some point after saturation. The sharp decrease in PL intensity seen in Figs. 3 and 5 can then be accounted for with a certain fraction of the islands becoming optically inactive, which happens with a sudden change in the ratio of incoherent/coherent islands.

The differences in PL intensity from QD's with 532- and 980-nm excitation (~ 30 times weaker with 980-nm excitation) that can be appreciated in Fig. 5 are consistent with previous experimental findings. Fafard *et al.*⁹ showed a large reduction in QD PL intensity with excitation below WL emission. The WL behaves as a reservoir of carriers that become available to the dots as long as the 2D diffusion length in the WL is large enough for capture to be possible, and as long as capture occurs before radiative recombination from WL states. This behavior suggests the possibility of using QD capture of carriers in the WL to obtain rough val-

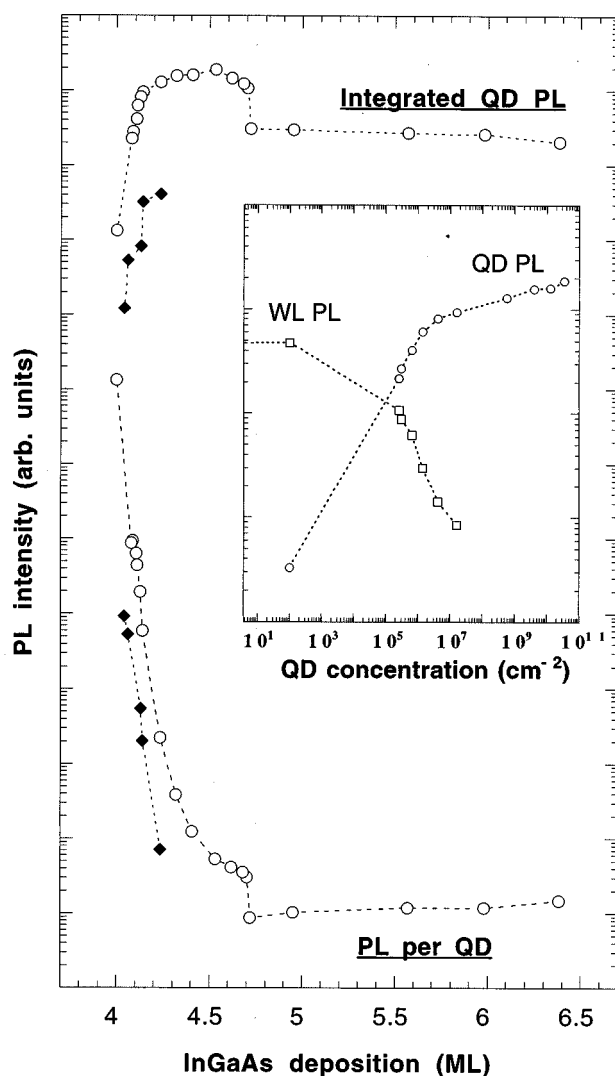


FIG. 5. Relative integrated PL intensity with above band-gap (532 nm) (open circles) and below band-gap (980 nm) (solid diamonds) excitation as a function of $\text{In}_x\text{Ga}_{1-x}\text{As}$ deposition. The inset shows relative integrated intensities from WL and QD luminescence as a function of QD concentration.

ues for 2D diffusion lengths in $\text{In}_x\text{Ga}_{1-x}\text{As}$ quantum structures. Threshold values of QD concentrations that produce a PL peak were used here to estimate upper ($2.5 \mu\text{m}$) and lower ($0.5 \mu\text{m}$) values for carrier 2D diffusion lengths in the $\text{In}_x\text{Ga}_{1-x}\text{As}$ wetting layer.

Figure 4 shows the PL spectra from various excitation powers over different regions of the evolution of island formation. The figure shows estimated dot concentrations. From the two lower groups it can be seen that the saturation behavior is dependent on QD concentration. The top group shows that the peak broadens with excitation power. The topmost curve was simulated by adding two Gaussian peaks with the same inhomogeneous broadening of 65 meV. It can thus be seen that the shoulder and broadening of the QD PL spectra at high excitation powers is from the ground state and first excited state emission from QD states. The peaks used in the simulation (shown in Fig. 4) are centered at 1.135 and 1.185 eV. This gives intersublevel spacings of 50 meV, a value in agreement with previous reports of intraband energies in similar $\text{In}_x\text{Ga}_{1-x}\text{As}/\text{GaAs}$ QD's.^{10,11}

In the lower two sets of curves in Fig. 4, an interesting behavior is seen in the radiative recombination when both WL and QD PL are detectable. As laser excitation power is increased, the WL peak increases more than the QD peak. This behavior can be easily explained by the fact that due to sharpened density of states, QD's saturate at much lower excitation than QW's. Another interesting observation from Figs. 4(b) and 4(c) is that QD luminescence saturates more readily for low QD concentrations. This sharpened 0D behavior might be due to the fact that at such low QD densities interdot interactions are nil.

To conclude, this optical and structural study of QD evolution has shown that once the islands/dots start forming, any extra deposited $\text{In}_x\text{Ga}_{1-x}\text{As}$ goes either into the preformed islands or into making new islands, and the wetting layer thickness stays constant. An abrupt drop in PL intensity is observed beyond saturation island densities. This drop in PL corresponds with a sudden increase in the concentration of incoherent islands. It was also found that while the integrated QD PL increases with QD concentration, it does not do so proportionally, so the intensity per QD drops as the concentration of QD's increases. QD saturation behavior also changes with dot concentration. The WL/QD intensity ratio increases with increased excitation intensity for lower QD concentrations.

The authors thank A. Clark for helpful discussions. Financial support from the Australian Research Council and from the Center for Integrated Space Microsystems (CISM) at the Jet Propulsion Laboratory is acknowledged.

*Present address: Jet Propulsion Laboratory, California Institute of Technology, 4800 Oak Grove Drive, Pasadena, CA 91109-8099.

¹R. P. Mirin, J. P. Ibbetson, K. Nishi, A. C. Gossard, and J. E. Bowers, *Appl. Phys. Lett.* **67**, 3795 (1995).

²J. C. Campbell, D. L. Huffaker, H. Deng, and D. G. Deppe, *Electron. Lett.* **33**, 1337 (1997).

³J. van de Ven, G. M. J. Rutten, M. J. Raaijmakers, and L. J. Giling, *J. Cryst. Growth* **76**, 354 (1986).

⁴D. Leonard, K. Pond, and P. M. Petroff, *Phys. Rev. B* **50**, 11 687 (1994).

⁵N. P. Kobayashi, T. R. Ramachandran, P. Chen, and A. Madhukar, *Appl. Phys. Lett.* **68**, 3299 (1996).

⁶D. J. Eaglesham, F. C. Unterwald, and D. C. Jacobson, *Phys. Rev. Lett.* **70**, 966 (1993).

⁷C. W. Snyder, B. G. Orr, and H. Munekata, *Appl. Phys. Lett.* **62**, 46 (1993).

⁸S. Fafard, Z. Wasilewski, and J. McCaffrey (unpublished).

⁹S. Fafard, D. Leonard, J. L. Merz, and P. M. Petroff, *Appl. Phys. Lett.* **65**, 1388 (1994).

¹⁰S. Fafard, R. Leon, D. Leonard, J. L. Merz, and P. M. Petroff, *Phys. Rev. B* **52**, 5752 (1995).

¹¹S. Raymond, S. Fafard, S. Charbonneau, R. Leon, D. Leonard, P. M. Petroff, and J. L. Merz, *Phys. Rev. B* **52**, 17 238 (1995).